	Experiment title: Local structure of novel dilute magnetic semiconductors	**Experiment number**: 26-01 1018
Beamline: BM26A	**Date of experiment**: from: 23 January 2015 to: 27 January 2015	**Date of report**: 01-04-2015
Shifts: 12	Local contact(s)**:** Dipanjan Banerjee	*Received at ESRF:*

Names and affiliations of applicants (* indicates experimentalists):

* Prof. Lino Pereira (KU Leuven, Belgium)
Prof. Kristiaan Temst (KU Leuven, Belgium)
Prof. André Vantomme (KU Leuven, Belgium)
Prof. Caroline Ross (MIT, USA)
* Koen Van stiphout (KU Leuven, Belgium)
* Valérie Augustyns (KU Leuven, Belgium)
* Tiago de Lemos Lima (KU Leuven, Belgium) - experimentalist, not applicant

Goal:

The experiment consisted of determining if and which secondary phases where formed in Fe-implanted $SrTiO_3$ for the implantation and annealing conditions that had been previously observed to result in ferromagnetic behavior, as well as for the annealing conditions that rendered the ferromagnetic samples non-ferromagnetic.

Samples:

sample ID	implanted element	ion fluence (at. /cm^2)	nominal concentration (%)	preceeding annealing step	annealing temperature ^{o}C	annealing environment (mbar)
S1	Fe	5E15	8	-	as-implanted	vacuum (~1E-6)
S2	Fe	1E16	16	-	as-implanted	vacuum (~1E-6)
S3	Fe	1.5E16	24	-	as-implanted	vacuum (~1E-6)
S4	Fe	5E15	8	-	500	vacuum (~1E-6)
S5	Fe	1E16	16	-	500	vacuum (~1E-6)
S6	Fe	1.5E16	24	-	500	vacuum (~1E-6)
S7	Fe	5E15	8	S4	900	vacuum (~1E-6)
S8	Fe	1E16	16	S5	900	vacuum (~1E-6)
S9	Fe	1.5E16	24	S6	900	vacuum (~1E-6)
S10	Fe	5E15	8	S7	900	air

S11	Fe	1E16	16	S8	900	air
S12	Fe	1.5E16	24	S9	900	air
S13	Fe	5E15	8	S10	900	vacuum (~1E-6)
S14	Fe	1E16	16	S11	900	vacuum (~1E-6)
S15	Fe	1.5E16	24	S12	900	vacuum (~1E-6)
S16	Fe	5E15	8	S4	1000	air
S17	Fe	1E16	16	S5	1000	air
S18	Fe	1.5E16	24	S6	1000	air
S19	Fe	5E15	8	S16	900	vacuum (~1E-6)
S20	Fe	1E16	16	S17	900	vacuum (~1E-6)
S21	Fe	1.5E16	24	S18	900	vacuum (~1E-6)

The samples (listed in the table above) consisted of commercial $SrTiO_3$ single-crystalline substrates, implanted with Fe (the implanted layer corresponds to the top ~40 nm) to three different nominal Fe concentrations *x* (8%, 16%, and 24%) corresponding to implanted fluences (areal densities) of 5×10^{15}, 1×10^{16} and 1.5×10^{16} at./cm^2, respectively. These concentrations were selected based on SQUID and Mössbauer spectroscopy measurements showing that: samples with x = 8% and x = 16% are ferromagnetic (after 700-900ºC annealing in vacuum ~1×10^{-6} mbar) but no magnetic secondary phases could be identified; samples with x = 24% show a distinct ferromagnetic behavior and metallic α-Fe could be identified by Mossbauer spectroscopy.

Results:

By combining these XAFS measurements with SR-XRD measurements at the BM20B beamline (ESRF), as well as STEM-EDX, SQUID magnetometry and Mössbauer spectroscopy, the observed ferromagnetism could finally be correlated with the presence of Fe-rich ferromagnetic or ferrimagnetic secondary nanophases. The change in magnetic behavior upon air annealing could be correlated with the oxidation of metallic phases or the change in O-stoichiometry of already oxide phases. We are **currently preparing two manuscripts associated with this experiment**:

1. On the identification of fcc Fe (γ-Fe) nanoparticles (for x = 8% and x = 16%), a phase that is thermodynamically unstable in bulk. Even more remarkably, the magnetic coupling within the nanoparticles is ferromagnetic, whereas common γ-Fe nanoparticles/thin-films (typically embedded/grown on Cu) are antiferromagnetic. These findings inspire a completely new type of artifical multiferroics (cf. *Outlook* below).
2. On the remarkably *reversible* oxidation-reduction of Fe-oxides which are normally very stable (e.g. the reduction of embedded Fe_2O_3 nanoparticles into metallic Fe by annealing in moderate vacuum at only 900ºC). These unexpected effects can be attributed to the low oxygen chemical potential in the $SrTiO_3$ layer surrounding the embedded Fe_2O_3 nanoparticles, resulting from the thermal annealing in vacuum which creates a significant concentration of oxygen vacancies (which in turn "absorb" oxigen atoms from the oxide nanoparticles).

Comment on statistics:

Due to the low amount of Fe in the samples, the EXAFS data was of limited quality, with a usable maximum k value of only 10 Å^{-1} (cf. Fig. 1 left). Nevertheless, by complementing the EXAFS data with the also measured XANES data (cf. Fig. 2, right) and the other techniques mentioned above (STEM-EDX, SQUID and Mössbauer), we were able to achieve a convincing analysis and interpretation.

Outlook:

As mentioned above in the context of manuscript 1 (in preparation), these findings open the way for studies on a completely new mechanism of strain-mediated magnetoelectric coupling in artificial multiferroics. We are currently investigating these effects, including a new proposal for further EXAFS experiments at BM26A (to be submitted by the April 2015 call), on samples which are specifically designed to overcome the limitations mentioned above (cf. *Comment on statistics*).

Additional (unforeseen) measurements:

Taking advantage of a beam time remainder of 5 hours, we measured four samples of a related material system: Fe-implanted $BiFeO_3$ thin films (200 nm). Given the significantly larger amount of Fe in these samples, we were able to collect good-quality EXAFS data, confirming the formation of Fe_2O_3 nanoparticles (also complemented by SR-XRD, SQUID magnetometry and Mössbauer spectroscopy). These measurements and analysis (Fig. 2) are included in a **third manuscript (in preparation) associated with this experiment**, dealing with the exchange-coupling between multiferroic $BiFeO_3$ (ferroelectric and antiferromagnetic) and the ferrimagnetic Fe_2O_3 nanoparticles.

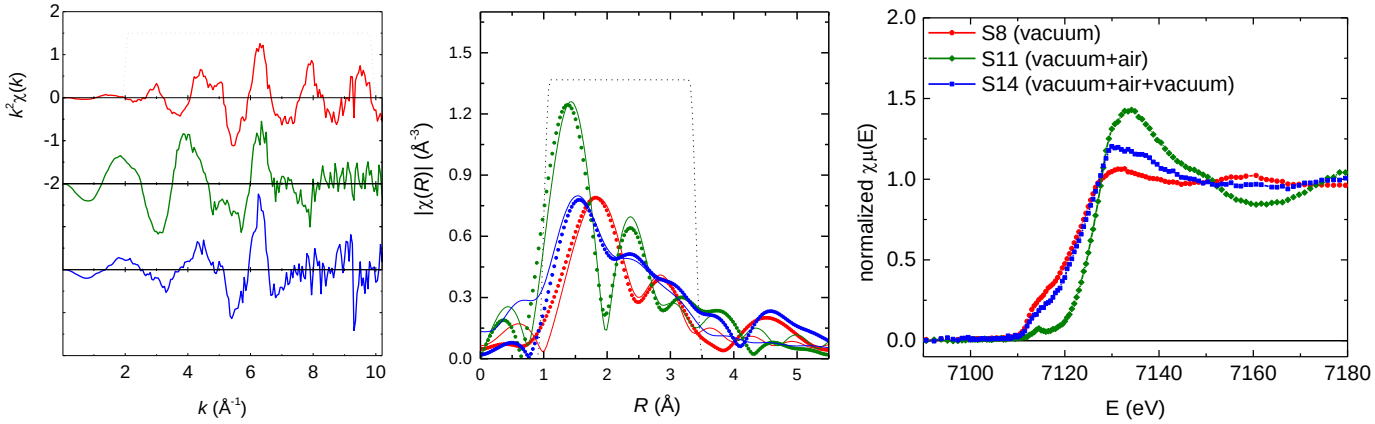

Fig. 1 – Selected data on Fe-implanted $SrTiO_3$ (samples S8, S11, and S14) showing the reversible oxidation-reduction mentioned above in the contex of manuscript 2. (Left) Spectra of k^2-weighted EXAFS. The dashed line represents the Hanning window used for the backward FT in the fitting procedure. (Center) Magnitude of the Fourier transform (symbols) as a function of non-phase corrected radial distance. The solid lines represent the best fit to the experimental data allowing for three fractions of Fe atoms: "dilute" in $Sr(Ti,Fe)O_3$, in γ-Fe, and in Fe_2O_3. The dashed line represents the Hanning window used for the backward FT in the fitting procedure. (Right) XANES data on the same samples (quantitative analysis is currently ongoing).

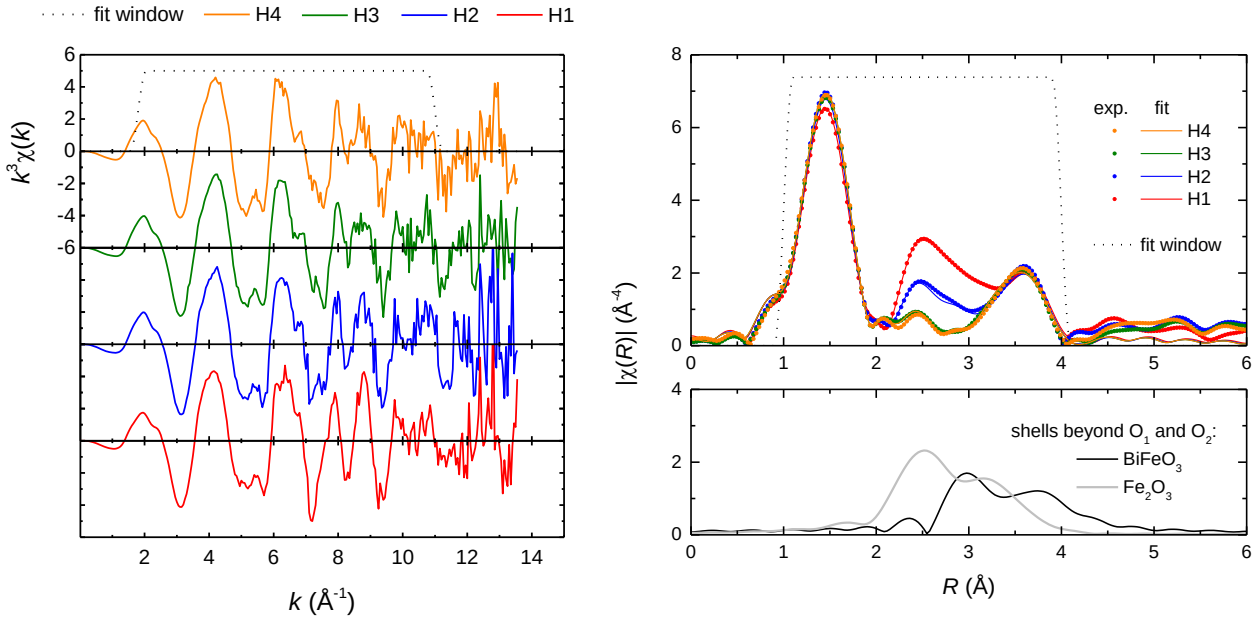

Fig. 2 – Data on Fe-implanted $BiFeO_3$. (Left) Spectra of k^3-weighted EXAFS. The dashed line represents the Hanning used for the backward FT in the fitting procedure. (Right, top) Magnitude of the Fourier transform (symbols) as a function of non-phase corrected radial distance. The solid lines represent the best fit to the experimental data allowing for two fractions of Fe atoms: in $BiFeO_3$ and in Fe_2O. (Right, bottom) Magnitude of the Fourier transform corresponding to the shells of order higher than that of the first and second nearest Oxygen neighbors (O_1 and O_2) in $BiFeO_3$ and in Fe_2O_3, illustrating how EXAFS discriminates de two components.